Measurement of Neutron-Production Double-Differential Cross Sections for High-Energy Pion-Incident Reaction

Yousuke IWAMOTO[1], Kiminori IGA[1], Hirohiko KITSUKI[1], Hideki TENZOU[1], Shunsuke ISHIMOTO[1], Nobuhiro SHIGYO[1], Keisuke MAEHATA[1], Kenji ISHIBASHI[1]

Tatsushi NAKAMOTO[2], Masaharu NUMAJIRI[2], Shin-ichiro MEIGO[3] and Hiroshi TAKADA[3]

1 Department of Applied Quantum Physics and Nuclear Engineering, Kyushu University

2 High Energy Accelerator Research Organization

3 Japan Atomic Energy Research Institute

email: yousuke@meteor.nucl.kyushu-u.ac.jp

Abstract

Double-differential neutron-production yields for 870-MeV π^+, π^- and 2.1-GeV π^+ incident on iron and lead targets were measured with NE213 liquid scintillators by time-of-flight technique. The two-gate integration method was used for the pulse shape discrimination between neutrons and gamma-rays. Neutron detection efficiencies were derived from the calculation results of SCINFUL and CECIL codes. The experimental results were compared with the calculation including the neutron transport in the actual thickness target by the contribution use of both NMTC/JAERI97 and MCNPX.

1. Introduction

Nuclear data in the intermediate energy region up to GeV-grade are recently getting more important because of necessity in applications to a spallation neutron source and an accelerator-based nuclear-waste transmutation system. For such applications, proton incident reactions are used for generating neutrons. At incident energies above 0.5 GeV, a number of pions are yielded from the primary proton reaction. The pions easily induce the secondary reactions, and accordingly create secondary neutrons in the target. Calculation codes such as High Energy Transport Code (HETC) [(1) (2)] are based on Birtini's intranuclear-cascade-evaporation (INCE) model [(3)]. These codes have been formed to be applicable to the nuclear reaction for both nucleon and meson incidences. The validity of the codes has been comfirmed by a comparison between the proton-incident experimental data and the computed ones. For neutron-production cross section by pion incidence, however, there are no experimental data at incident energies around 1GeV. The INCE model has not been checked for neutron-production double-differential cross section on the intermediate-energy pion-incident nuclear reaction. Therefore, we measured the double-differential yields for 870-MeV (momentum of 1.0GeV/c) $\pi+, \pi-$ mesons and 2.1-GeV (that of 2.25GeV/c) $\pi+$ mesons incident on iron and lead. In this work, we describe the experimental method and the data analysis.

2. Experiment

2.1 Incident Pion Beam

The experiments were carried out at the $\pi 2$ beam line of the 12GeV proton synchrotron (12GeV-PS) at High Energy Accelerator Research Organization (KEK). The experimental arrangement is illustrated in **Fig.1**. Since the beam intensity was very weak, the pions were able to be individually counted one by one. Incident pions were generated in a secondary beam from an internal target mounted in the accelerator ring. The secondary beam contains several kinds of particles. In selection of positive beam polarity, unresolved particles of π^+, proton, μ^+ and positron come together with the same momentum, whereas π^-, electron and μ^- are available at negative polarity. At a momentum of 1GeV/c, the fractions of μ and positron are less than several percents. For positive beam incidence, the Time-of-Flight (TOF) of incident particles was measured for separation of protons from π^+ mesons and other lighter particles by the use of a pair of Pilot U scintillators. These scintillators were located at beam line with a flight distance of 4.5m. Time differences between π^+ and protons are 4.9 and 1.07ns at momentums of 1.0 and 2.25GeV/c, respectively. Since the time resolution was 0.29ns for the incident-beam TOF measurement, protons were well separated by the electronic circuit. We set up a Cerenkov counter at the beam line to separate π^+ (π^-) from μ^+ and positron (μ^- and electron) by means of the difference of Cerenkov light emission. NE102A plastic scintillators served to define the pion beam with Pilot U scintillators. The coincidence of these scintillators was counted to give the number of incident pions.

2.2 Target and Detector Arrangement

A target was located at beam line height of 1.0m and all neutron detectors were faced to the target. A iron target was 4.9cm in diameter and 3.0cm thick, while a lead target 4.9cm in diameter and 1.7cm thick. Since the targets were not quit thin, we had to take correction of multiple-scattering effects into consideration.

For neutron TOF measurements, NE213 neutron detectors 12.7cm in diameter and 12.7cm thick were placed in directions of 15, 30, 60, 90, 120 and 150^o, as indicated in **Fig.1** . Flight pass lengths were 1.5 to 2m. The scintillators were connected with Hamamatsu H1161. In front of individual neutron detectors, NE102A plastic scintillators 1cm thick were mounted as veto detectors to eliminate charged particle events by the anticoincidence method.

2.3 Pulse-Shape Discrimination

It was very important to perform the pulse-shape discrimination between neutrons and gamma rays particularly in the short flight path experiment. This is because prompt gamma-rays peak are not completely separated from neutron events in the TOF spectra. For the pulse-shape discrimination method, there are mainly two methods, the zero-cross method [4] [5] [6] [7] and the two-gate integration method [8] [9] [10]. It was known that the latter is capable of reducing the saturation effect on the neutron-gamma discrimination in the high-energy region. The two-gate integration method was chosen for this experiment. For this reason, the photomultiplier signal was branched into two pulses and they were input into individual ADCs as fast or slow gate pulses. The prompt gate on one ADC covered the initial peak of the photomultiplier signal, whereas the delayed gate made the other ADC to accept the long-tail part. The time duration of the prompt gate was 40 ns and that of the delayed gate was 350 ns after

delay of 150 ns. The discrimination results of 870MeV π^+ on Fe target are shown in **Fig.2**. The discrimination characteristics were sufficiently good above a few MeV and the saturation effect did not deteriorate the discrimination results.

3. Data Analysis

Target-in and -out experiments were performed in the neutron measurements. Neutron spectra were derived by subtracting the results of target-out experiment from those of the target-in with normalizing the incident number of pions. **Fig.3** presents the TOF spectra of the target-in and -out measurements at incident π^+ energy of 870MeV on iron. In this figure, the pulse-shape discrimination was not made and the TOF spectra include both of neutrons and gamma-rays. The flash gamma-rays which emitted from target nuclei exited by incident pions make a peak at 156ns. The flash gamma-ray peak was taken as the time standard of the neutron TOF, since the gamma-rays came along on the flight path as the light velocity. The TOF of neutrons is given as the time difference between flash gamma-rays and neutrons. The neutron production double differential yields were extracted from the neutron TOF spectra, which were separated from gamma-rays by the pulse-shape discrimination. The number of neutron events were converted into the differential cross sections by using the efficiencies of the neutron detectors and making the data corrections.

3.1 Neutron Detection Efficiencies

Neutron detection efficiencies are required to convert the neutron events into absolute values of the cross sections. It is desired to adopt the measured detection efficiencies to the data analysis. However, it was difficult to measure the neutron detection efficiencies in the neutron energy range up to a GeV. The neutron detection efficiencies were obtained from calculation results of the SCINFUL [(11)] and the CECIL [(12)] codes. SCINFUL is well known to reproduce the detection efficiencies of the NE213 and NE110 scintillators at neutron energies below 80MeV. SCINFUL is supposed to be more reliable than CECIL in this region. In fact, SCINFUL takes account of many reaction channels for n+C reaction and light output values for all charged particles generated by this reaction. For this reason, SCINFUL was utilized for the neutron detection efficiencies below 80MeV. CECIL was adjusted to smoothly connect with the result of the SCINFUL at 80MeV and was employed above 80MeV.

The neutron detection efficiencies were calculated with four threshold levels. Calculation results of the neutron detection efficiencies with the four threshold levels are plotted in **Fig.4**. The lowest threshold level was determined by the photo-peak of 60keV gamma-rays from ^{241}Am. The other threshold levels were determined by the half-height of the Compton edge produced by radiation source by ^{137}Cs, ^{60}Co, and Am-Be. In the case of ^{60}Co bias, we adopted the mean value of 1.17 and 1.33 MeV gamma-rays as the threshold level because the poor resolution of the NE213 scintillator made these Compton edges unresolved.

4. Double differential yield

The experimental neutron yields were obtained after data analysis. The yields was presented in units of double differential neutron cross sections for iron and lead are plotted in **Figs. 5** to **9**. Solid lines show the calculation

results including the neutron transport in the actual thickness target by the use of nucleon-meson transport code (NMTC/JAERI97) [13] and MCNPX code[14]. The neutron transport at energies below 150MeV was made by MCNPX with a continuous energy cross section library, which were processed from the nuclear data of ENDF-B/VI and an additional data base. The calculation results overestimate the experimental data in the neutron energy range from 3 to 50 MeV in all degrees. Compared with iron and lead targets, the agreement between the experimental data and calculation ones for lead is somewhat better than iron in the energy range from 3 to 50 MeV. The experimental data for 870MeV π^- incidence are better agreement with the calculation ones than π^+ incidence above 100MeV, and the experimental ones for 2.1GeV π^+ incidence better agree with the calculation ones than 870MeV π^+ incidence.

The difference between yields and cross sections is within about 10% under 50MeV. We will take into the actual beam profile consideration. After correction of the beam transport effects in the target, the double differential cross sections will be obtained.

5. Conclusion

Neutron-production double-differential yields induced by 870MeV π^+, π^- mesons and 2.1 GeV π^+ meson on iron and lead targets were obtained in the emitted neutron energy range from 1 MeV to 1 GeV by the TOF method with a typical flight pass length of 1.5 m. NE213 liquid scintillators were utilized in directions of 15, 30, 60, 90, 120 and 150 ° for the measurements. For the pulse-shape discrimination between neutron and gamma-ray, the two-gate integration method was used. Neutron detection efficiencies were derived from the calculation results of the SCINFUL and the CECIL codes. The effects of multiple-scattering neutrons will be corrected later.

Acknowledgements

The authors express their gratitude to Prof. Y. Yoshimura and beam channel staff of KEK for their continuous encouragement and generous support of this experiment.

Reference

(1) CHANDLER, K. C., ARMSTRONG, T. W.: *CCC*-178, (1977).

(2) COLEMAN, W. A., ARMSTRONG, T. W.: *ORNL*-4606, (1970).

(3) BERTINI, H. W., et al.: *Phys. Rev.*, **188**, 1711 (1969).

(4) BROOKS, F. D., *Nucl. Instrum. Methods* **4**, 151 (1959)

(5) MCBETH, G. W., LUTKIN, J.E. and WINYARD, R. A., *Nucl. Instrum. Methods* **93**, 99 (1971)

(6) GLASGOW, D. W., VELKLEY, D. E., BRANDENBERGER, J. D. and MCELLISTREM, M. T., *Nucl. Instrum. Methods* **136**, 579 (1976)

(7) PLISCHKE, P., SCHRODER, V., SCOBEL, W., WILDE, L. and MCELLISTREM, M. T., *Nucl, Instrum. Methods* **114** 535 (1974)

(8) BELL, Z. W., *Nucl. Instrum. Methods* **188**, 105 (1981)

(9) ZUCKER, M. S. and TSOUPAS, N., *Nucl. Instrum. Methods* A **299**, 281 (1990)

(10) MOSZYNSKI, M., et al., *Nucl. Instrum. Methods* A **343**, 563 (1994)

(11) DICKENS, J. K., ORNL-6452 (1988)

(12) CECIL, R. A., et al., *Nucl. Instr. And Meth.*, **161**, 439 (1979)

(13) TAKADA, H., et al., *JAERI-DATA/CODE* 98-005 (1998)

(14) BRIESMEISTER, J.F, et al., *LA*-12625-*M* (1997)

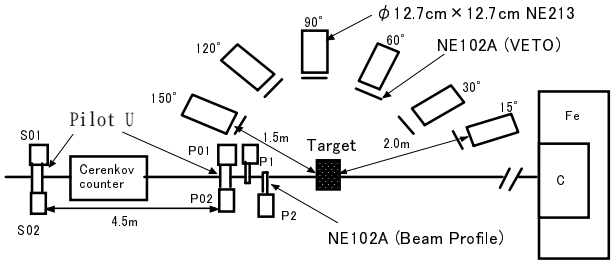

Fig.1 Illustration of the experimental arrangement

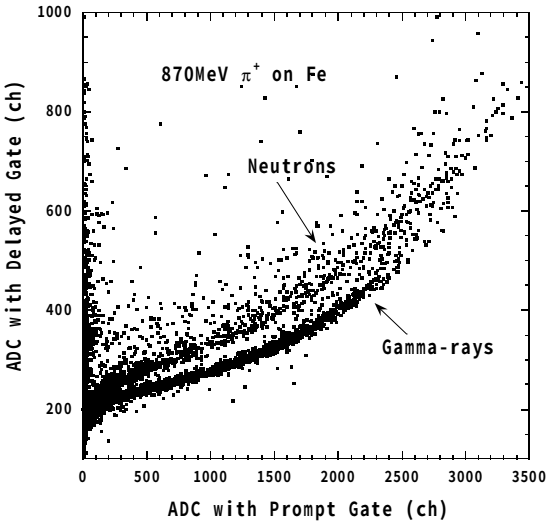

Fig. 2 Neutron and gamma-ray pulse-shape discrimination by two-integration method.

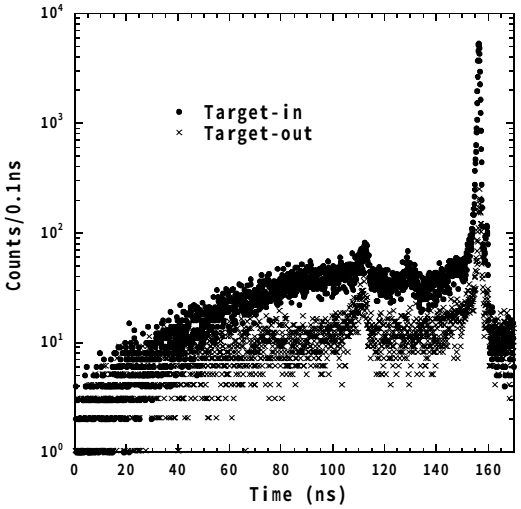

Fig. 3 TOF spectra of the target-in and -out measurements at 30° for 870 MeV π^+ on Fe.

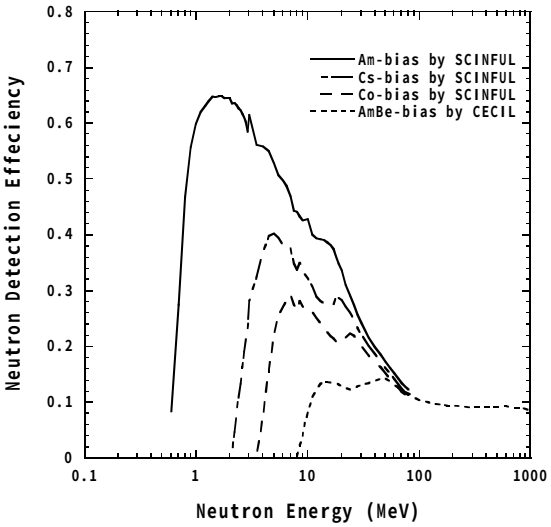

Fig. 4 Calculated neutron detection efficiencies for NE213 liquid scintillatos.

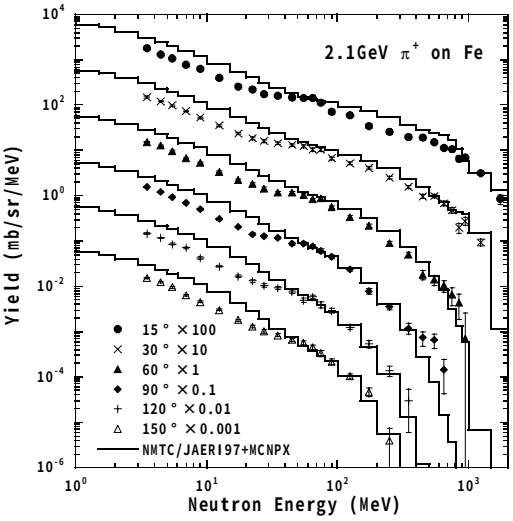

Fig. 5 Neutron production double differential yield for 2.1GeV π^+ on Fe.

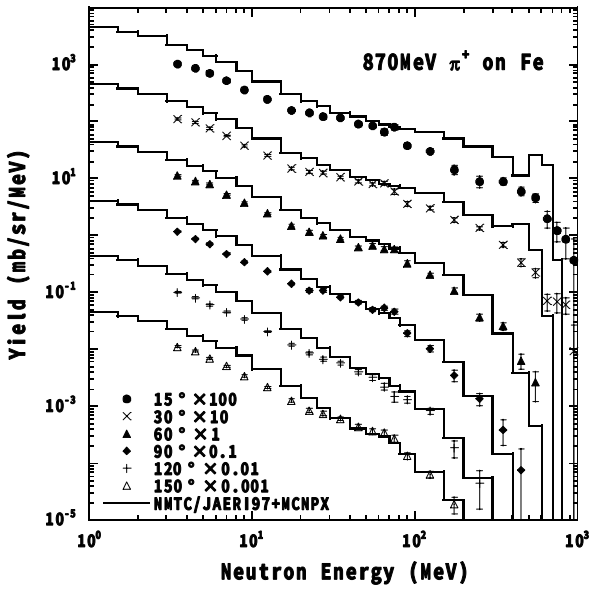

Fig. 6 Neutron production double differential yield for 870MeV π^+ on Fe.

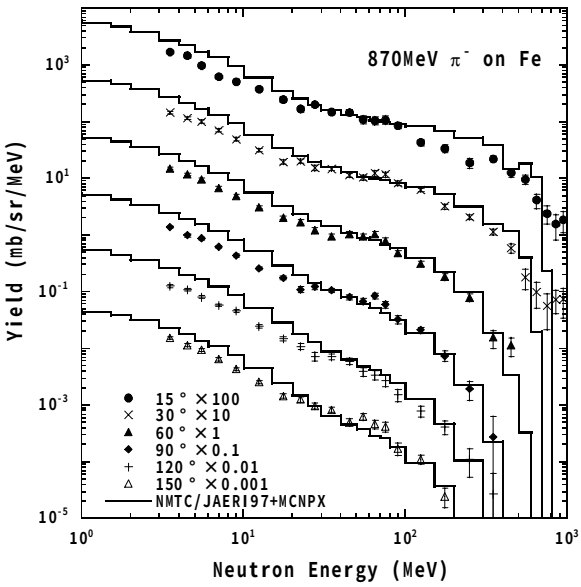

Fig. 7 Neutron production double differential yield for 870MeV π^- on Fe.

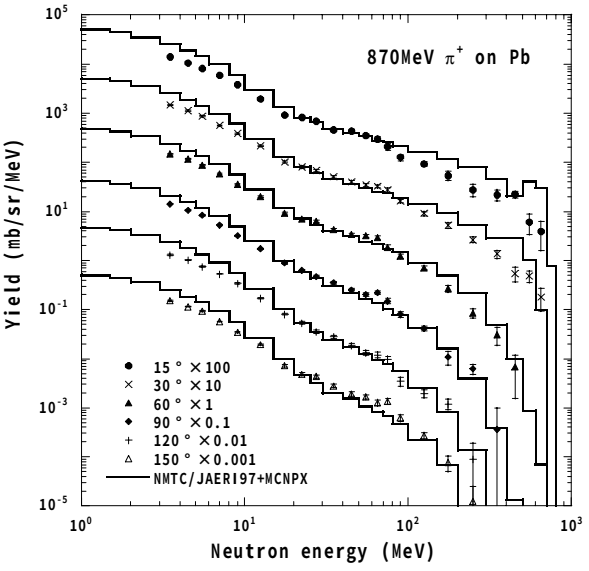

Fig. 8 Neutron production double differential yield for 870MeV π^+ on Pb.

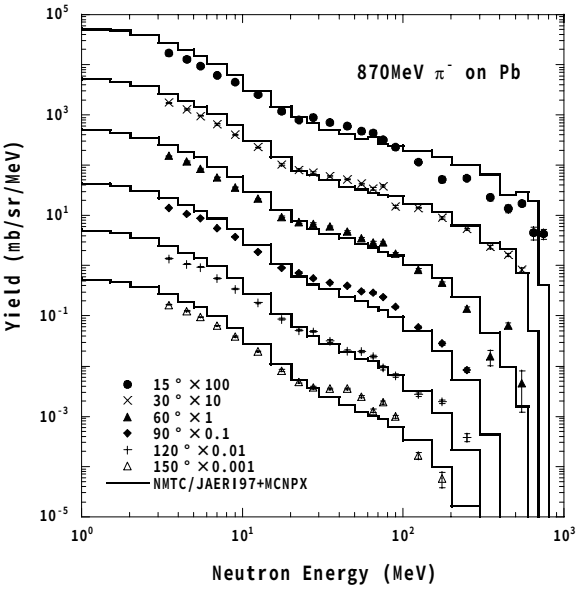

Fig. 9 Neutron production double differential yield for 870MeV π^- on Pb.